Flexible energy storage devices based on nanocomposite paper

Victor L. Pushparaj*, Manikoth M. Shaijumon*, Ashavani Kumar*, Saravanababu Murugesan†, Lijie Ci*, Robert Vajtai‡, Robert J. Linhardt†, Omkaram Nalamasu*, and Pulickel M. Ajayan*‡§

Departments of *Materials Science and Engineering and †Chemical and Biological Engineering, and Center for Biotechnology and Interdisciplinary Studies, ‡Rensselaer Nanotechnology Center; Rensselaer Polytechnic Institute, Troy, NY 12180

Communicated by Mildred S. Dresselhaus, Massachusetts Institute of Technology, Cambridge, MA, July 11, 2007 (received for review February 23, 2007)

There is strong recent interest in ultrathin, flexible, safe energy storage devices to meet the various design and power needs of modern gadgets. To build such fully flexible and robust electrochemical devices, multiple components with specific electrochemical and interfacial properties need to be integrated into single units. Here we show that these basic components, the electrode, separator, and electrolyte, can all be integrated into single contiguous nanocomposite units that can serve as building blocks for a variety of thin mechanically flexible energy storage devices. Nanoporous cellulose paper embedded with aligned carbon nanotube electrode and electrolyte constitutes the basic unit. The units are used to build various flexible supercapacitor, battery, hybrid, and dual-storage battery-in-supercapacitor devices. The thin freestanding nanocomposite paper devices offer complete mechanical flexibility during operation. The supercapacitors operate with electrolytes including aqueous solvents, room temperature ionic liquids, and bioelectrolytes and over record temperature ranges. These easy-to-assemble integrated nanocomposite energy-storage systems could provide unprecedented design ingenuity for a variety of devices operating over a wide range of temperature and environmental conditions.

batteries | carbon nanotubes | supercapacitor

There has been recent interest in flexible safe energy devices, based on supercapacitors and batteries, to meet the various requirements of modern gadgets (1–3). Electrochemical energy can be stored in two fundamentally different ways. In a battery, the charge storage is achieved by electron transfer that produces a redox reaction in the electroactive materials (3). In an electric double-layer capacitor, namely the supercapacitor, the charge-storage process is nonFaradic, that is, ideally no electron transfer takes place across the electrode interface, and the storage of electric charge and energy is electrostatic. Because the charging and discharging of such supercapacitors involve no chemical phase and composition changes, such capacitors have a high degree of cyclability. However, in certain supercapacitors based on pseudocapacitance, the essential process can be Faradic, similar to that in a battery. However, an essential fundamental difference from battery behavior arises because, in such systems, the chemical and associated electrode potentials are a continuous function of degree of charge, unlike the thermodynamic behavior of single-phase battery reactants (3). Now, with the demand for efficient power devices to meet the high-power and -energy applications, there seems to be the possibility of an ideal compromise, which combines some of the storage capabilities of batteries and some of the power-discharge characteristics of capacitors in devices capable of storing useful quantities of electricity that can be discharged very quickly. We address here this need to develop new integrated hybrid devices with adaptability in various thin-film as well as bulk applications by using engineered electrode nanostructures.

The performance characteristics of energy devices are fundamentally determined by the structural and electrochemical properties of electrode materials (4–7). Electrolyte choice (aqueous vs. nonaqueous), limiting high-power capability and packaging designs, is the other important factor in supercapacitors and batteries (8, 9). If integrated structures containing the three essential components (electrodes, spacer, and electrolyte) of the electrochemical device can be made mechanically flexible, it would enable these to be embedded into various functional devices in a wide range of innovative products such as smart cards, displays, and implantable medical devices. Previous designs of flexible energy-storage devices (1) have been based on separated thin-electrode and spacer layers, proving less-than-optimum in performance and handling because of the existence of multiple interfaces between the layers. Here we demonstrate the fabrication of electrode-spacer-electrolyte-integrated nanocomposite units to build a variety of thin flexible energy-storage devices. We combine two essential materials, cellulose and carbon nanotubes (CNTs), that fit the characteristics of spacer and electrode and provide inherent flexibility as well as porosity to the system. Cellulose, the main constituent of paper and a inexpensive insulating separator structure with excellent biocompatibility, can be made with adjustable porosity. CNTs, a structure with extreme flexibility, have already been widely used as electrodes in electrochemical devices (10–16). The major challenge in fabricating CNT-integrated cellulose composites is the insolubility of cellulose in most common solvents. This issue is solved here by using a room temperature ionic liquid (RTIL) (17) 1-butyl,3-methylimidazolium chloride ([bmIm][Cl]) (17), which dissolves up to 25% (wt/wt) of unmodified cellulose by using microwave irradiation (18). Interestingly, the ionic nature of RTIL (19) permits it be used as an electrolyte in supercapacitors (20), allowing the assembly of all three components (Fig. 1) via a simple scalable process.

Uniform films of vertically aligned thin-walled multiwalled nanotubes (MWNT) are grown on silicon substrates by using a thermal-chemical vapor-deposition method [supporting information (SI)]. Unmodified plant cellulose dissolved in RTIL ([bmIm][Cl]) (17) is infiltrated into the MWNT to form a uniform film of cellulose and [bmIm][Cl], embedding the MWNT (Fig. 1*a*). After solidification on dry ice, this nanocomposite is immersed in ethanol to partially or completely extract excess RTIL and dried *in vacuo* to remove residual ethanol. The resulting nanocomposite paper (Fig. 1*b*), which forms the basic building unit in our devices, is peeled from the substrate for use as the supercapacitor. The excellent mechanical flexibility of the nanocomposite paper (CNT cellulose–RTIL) is shown in Fig. 1*b*.

Author contributions: V.L.P., M.M.S., A.K., R.J.L., O.N., and P.M.A. designed research; V.L.P., M.M.S., A.K., and S.M. performed research; V.L.P., A.K., S.M., L.C., and R.V. contributed new reagents/analytic tools; V.L.P., M.M.S., R.J.L., O.N., and P.M.A. analyzed data; and V.L.P., M.M.S., and P.M.A. wrote the paper.

The authors declare no conflict of interest.

Abbreviations: CNT, carbon nanotube; [bmIm][Cl], 1-butyl,3-methylimidazolium chloride; MWNT, multiwalled nanotubes; RTIL, room temperature ionic liquid.

§To whom correspondence should be addressed. E-mail: ajayan@rpi.edu.

This article contains supporting information online at www.pnas.org/cgi/content/full/0706508104/DC1.

© 2007 by The National Academy of Sciences of the USA

Downloaded at Palestinian Territory, occupied on December 13, 2021

www.manaraa.com

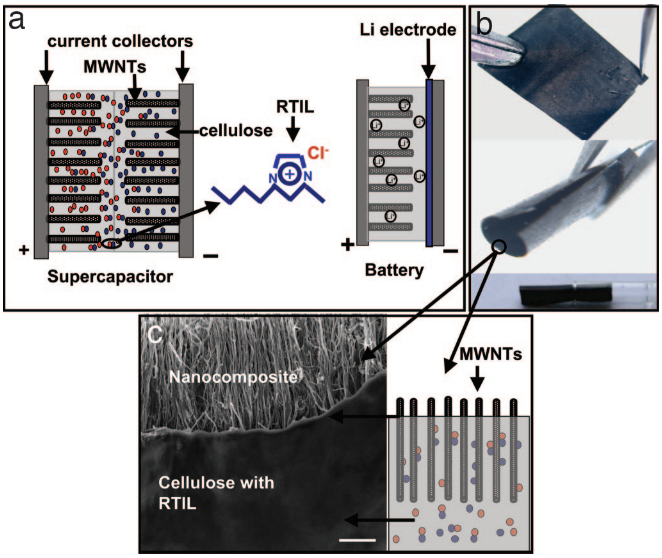

Fig. 1. Fabrication of the nanocomposite paper units for supercapacitor and battery. (*a*) Schematic of the supercapacitor and battery assembled by using nanocomposite film units. The nanocomposite unit comprises RTIL ([bmIm][Cl]) and MWNT embedded inside cellulose paper. A thin extra layer of cellulose covers the top of the MWNT array. Ti/Au thin film deposited on the exposed MWNT acts as a current collector. In the battery, a thin Li electrode film is added onto the nanocomposite. (*b*) Photographs of the nanocomposite units demonstrating mechanical flexibility. Flat sheet (top), partially rolled (middle), and completely rolled up inside a capillary (bottom) are shown. (*c*) Cross-sectional SEM image of the nanocomposite paper showing MWNT protruding from the cellulose–RTIL thin films. (Scale bar, 2 μm.) The schematic displays the partial exposure of MWNT.

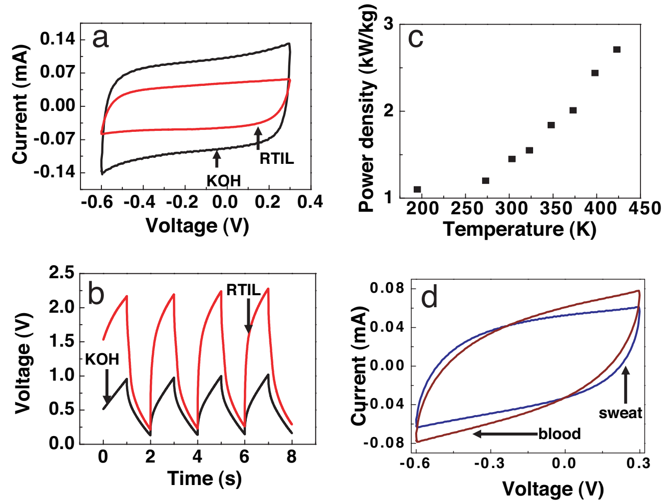

Fig. 2. Electrochemical double-layer capacitance measurements of nanocomposite paper supercapacitor. (*a*) Cyclic voltammograms (CV) and (*b*) charge–discharge behavior of the nanocomposite supercapacitor devices with KOH and RTIL electrolytes. The CV measurements are carried out at a scan rate of 50 mV/s at room temperature. The near-rectangular shape of the CV curves indicates good capacitive characteristics for the device. Charge–discharge behavior was measured at a constant current of 1 mA. (*c*) Power density of the supercapacitor device (using the RTIL electrolyte) as a function of operating temperature. The supercapacitor operates over a record range of temperatures (195–450 K). (*d*) CV of the supercapacitor by using bioelectrolytes [body fluids (blood, sweat)] measured at a scan rate of 50 mV/s at room temperature.

The paper can be rolled up, twisted, or bent to any curvature and is completely recoverable. Fig. 1*c* shows the cross-sectional SEM image of the nanocomposite with its corresponding structure. The cellulose is porous with randomly distributed pores of 50 ± 5 nm (21). The nanocomposite paper, which can be typically a few tens of microns thick, contains MWNTs as the working electrode and the cellulose surrounding individual MWNTs, as well as the extra layer as the spacer and the RTIL in cellulose as the self-sustaining electrolyte. Two of the nanocomposite units bonded back-to-back make a single supercapacitor device. The thin lightweight ($\approx$15-mg/cm^2) design of the device results from avoiding the use of a separate electrolyte and spacer, generally used in conventional supercapacitors. The use of RTIL electrolyte ($\approx$3 wt/wt % of cellulose in RTIL) makes the device environmentally friendly. In a final package, operating devices can be fabricated by laminating multiple stacks of individual nanocomposite layers (SI).

Results and Discussion

Electrochemical measurements were carried out for the supercapacitor and, in addition to using the nonaqueous RTIL electrolyte, 6 M KOH aqueous electrolyte was used to compare the performance. Fig. 2 *a* and *b* show good capacitive behavior of the supercapacitor by using aqueous (6 M KOH) and nonaqueous (RTIL) electrolytes. Devices using the KOH electrolyte showed lower equivalent series resistance compared with that with RTIL electrolyte. The CNT cellulose–RTIL nanocomposite showed a higher operating voltage ($\approx$2.3 V) compared with those with the KOH electrolyte ($\approx$0.9 V). The calculated specific capacitances were 36 F/g and 22 F/g for these devices with KOH and RTIL electrolytes, respectively. The specific capacitance of the device in the KOH solution is higher compared with RTIL, because the dielectric constant and ionic mobility of the latter are lower (22). A power density of 1.5 kW·kg^{-1} (energy density, $\approx$13 Wh/kg) is obtained at room temperature for the nanocomposite (RTIL) supercapacitor, which are within reported ranges (0.01–10 kW·kg^{-1}) of commercial supercapacitors and comparable to flexible devices reported (3).

The performance of supercapacitor (with RTIL) was next examined as a function of temperature to show the thermomechanical robustness of the device. The supercapacitor device, operated at different temperatures (195–450 K), shows a power density that increases with temperature (Fig. 2*c*), because of enhanced ionic conductivity. Although commercially available supercapacitors are reported to work typically in a temperature range of 233–358 K, our nanocomposite supercapacitor device showed a much wider record-operating temperature range (195–423 K). Cyclability testing was also carried out at various temperatures, and the device showed good performance over 100 cycles of charge and discharge. When measurement was performed at 77 K, the device showed no capacitive behavior but promptly recovered when returned to room temperature, demonstrating it device was not damaged when kept at ultralow temperatures (77 K).

In addition to using the aqueous and RTIL electrolytes, the device operates with a suite of electrolytes based on bodily fluids, suggesting the possibility of the device being useful as a dry-body implant or for use under special circumstances. As a precedent, a urine-activated battery was recently demonstrated for bio-MEMS device applications (23). Body sweat, composed of water, Na^+, Cl^-, and K^+ ions (24), used as electrolyte (a drop of sweat placed on the film gets sucked into the porous cellulose) in the RTIL-free nanocomposite affords good capacitive behavior for the device (specific capacitance of 12 F/g, operating voltage of $\approx$2.4 V; Fig. 2*d*). Blood (human whole blood in K_2 EDTA from Innovative Research, Southfield, MI) worked even better as an electrolyte, enhancing the capacitive behavior of the supercapacitor, resulting in a specific capacitance of 18 F/g (Fig. 2*d*).

ENGINEERING

Downloaded at Palestinian Territory, occupied on December 13, 2021

www.manaraa.com

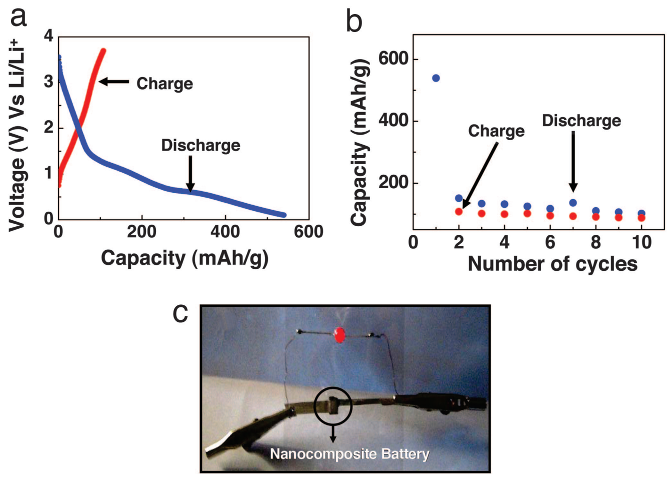

Fig. 3. Electrochemical measurements of nanocomposite paper battery. (*a*) First charge–discharge curves of the nanocomposite thin-film battery cycled between 3.6 and 0.1 V at a constant current of 10 mA/g. (*b*) Charge capacity vs. number of cycles of the nanocomposite thin-film battery. (*c*) The flexible nanocomposite film battery used to glow a red light-emitting diode (LED). The flexible battery consists of an individual nanocomposite thin film with the Li thin film present on one side as one of the electrodes. The LED glows even when the battery device is rolled up, and the demonstration could be repeated over several tens of cycles at an initial operating voltage of 2.1 V.

The fabrication of the flexible Li-ion battery based on the nanocomposite paper consists of RTIL-free nanocomposite as cathode and a thin evaporated Li-metal layer as anode (Fig. 1*a*), with Al foil on both sides as current collectors. Aqueous 1 M $LiPF_6$ in ethylene carbonate and dimethyl carbonate (1:1 vol/vol) is used as the electrolyte. As with the supercapacitor, the battery also uses the excess cellulose layer in the nanocomposite cathode as the spacer, without the use of any stand-alone spacer. The charge–discharge cycles of the battery were measured between 3.6 and 0.1 V, at a constant current of 10 mA/g. A large irreversible-capacity (≈430 mAh/g) is observed during the first charge–discharge cycle (Fig. 3*a*), and further charge–discharge cycles resulted in a reversible capacity of 110 mAh/g (Fig. 3*b*; see SI). The battery device operates under full mechanical flexibility. The laminated Li-ion-based battery device was used to light up a red light-emitting diode (Fig. 3*c*), showing its discharge behavior. The demonstration could be repeated over several tens of cycles of charging and discharging.

In recent years, supercapacitors coupled with batteries have been considered as promising hybrid devices (25, 26) to combine the best features of a battery and a supercapacitor. We show that our battery and supercapacitor devices could be integrated in parallel to build hybrids, as reported for conventional hybrids (Fig. 4*a*). In this case, the battery segment of the hybrid is used to charge the adjoining supercapacitor. In addition to this traditional hybrid, the nanocomposite units also allow for building new kinds of merged hybrid devices (27) (with three terminals; Fig. 4*b*, see legend for the definition of the terminals), which would act as both battery and supercapacitor (a dual-storage device). The Li metal layer (anode; terminal 2) and RTIL-free nanocomposite film (cathode; terminal 3) with a drop of aqueous electrolyte (1 M $LiPF_6$) forms the battery part of the hybrid, whereas the nanocomposite unit [MWNT (terminal 1)–cellulose–RTIL] assembled adjacent to the battery on the side of the Li layer forms the supercapacitor between terminals 1 and 3. During the operation of the device, the Li electrode (terminal 2) and the supercapacitor electrode (terminal 1) are shorted, and the discharge of the battery is used to charge the supercapacitor. The charging of the supercapacitor takes place because of intercalation at terminal 2; a PF_6^- double layer forms on the surface of the battery cathode (terminal 3), in addition to the electric double layer formed at the supercapacitor electrode

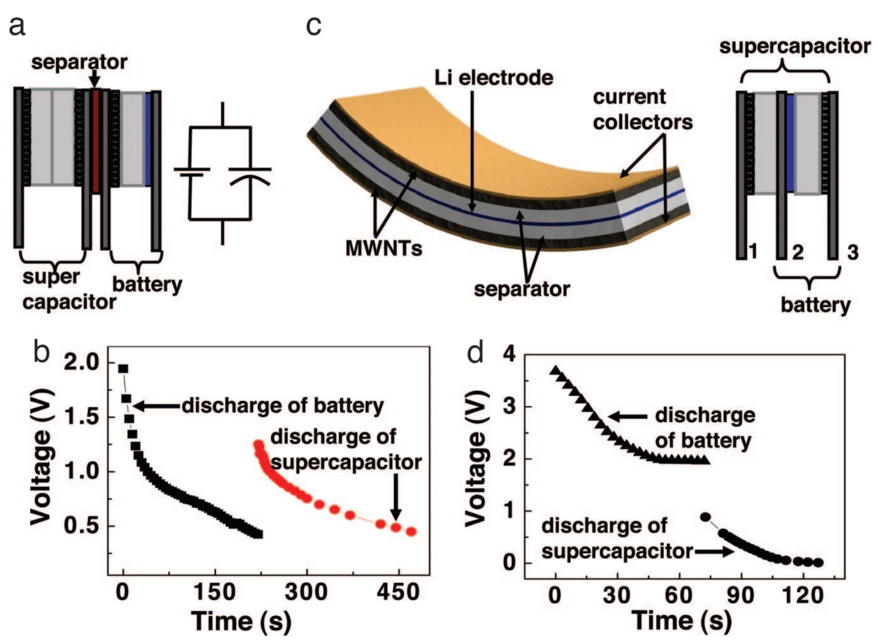

Fig. 4. Supercapacitor-battery hybrid energy devices based on nanocomposite units. (*a*) Schematic of a four-terminal hybrid-energy device showing the arrangement of supercapacitor and battery in parallel configuration. (*b*) The discharge curve of battery and supercapacitor is plotted as a function of time. The discharge of battery charges the supercapacitor, and subsequently the supercapacitor is discharged. (*c*) Schematic of a three-terminal hybrid energy device that can act as both supercapacitor and battery. The three terminals are defined, and the battery and supercapacitor segments of the device are shown. (*d*) The discharge behavior of the battery and subsequent discharge of supercapacitor are shown. The battery is discharged with terminals 1 and 2 shorted. This simultaneously charges the supercapacitor following the double-layer formation at the electrode interface. Subsequently, the supercapacitor is discharged across terminals 1 and 3. An additional separator (glass fibers) is normally added along with the excess cellulose spacer to improve behavior.

Downloaded at Palestinian Territory, occupied on December 13, 2021
www.manaraa.com

(terminal 1). The electric double layers (between terminals 1 and 3) in the supercapacitor can be discharged later in the supercapacitor mode. Hence the device acts as both supercapacitor and battery, a true hybrid, in comparison to the conventional hybrid shown in Fig. 4*a*.

Conclusion

To conclude, we have demonstrated the design, fabrication, and packaging of flexible CNT–cellulose–RTIL nanocomposite sheets, which can be used in configuring energy-storage devices such as supercapacitors, Li-ion batteries, and hybrids. The intimate configuration of CNT, cellulose, and RTIL in cellulose help in the efficient packaging, operation, and handling of these devices. The discharge capacity and performance observed here compare well with other flexible energy-storage devices reported (12). The robust integrated thin-film structure allows not only good electrochemical performance but also the ability to function over large ranges of mechanical deformation and record temperatures and with a wide variety of electrolytes. These selfstanding flexible paper devices can result in unprecedented design ingenuity, aiding in new forms of cost-effective energy storage devices that would occupy minimum space and adapt to stringent shape and space requirements.

We acknowledge funding support from the New York State Office of Science, Technology, and Academic Research (NYSTAR) and the National Science Foundation-funded Nanoscale Science and Engineering Center on directed assembly of nanostructures.

1. Sugimoto W, Yokoshima K, Ohuchi K, Murakami Y, Takasu Y (2006) *J Electrochem Soc* 153:A255–A260.
2. Nam KT, Kim DW, Yoo PJ, Chiang CY, Meethong N, Hammond PT, Chiang YM, Belcher AM (2006) *Science* 312:885–888.
3. Conway BE (1999) *Electrochemical Capacitors: Scientific Fundamentals and Technological Applications* (Kluwer, Dordrecht, The Netherlands).
4. Burke A (2000) *J Power Sources* 91:37–50.
5. Tarascon JM, Armand M (2001) *Nature* 414:359–367.
6. Dresselhaus MS, Thomas IL (2001) *Nature* 414:332–337.
7. Arico AS, Bruce P, Scrosati B, Tarascon JM, Van Schalkwijk W (2005) *Nat Mater* 4:366–377.
8. Hammami A, Raymond N, Armand M (2003) *Nature* 424:635–636.
9. Rose MF, Johnson C, Owens T, Stephens B (1994) *J Power Sources* 47:303–312.
10. Niu CM, Sichel EK, Hoch R, Moy D, Tennent H (1997) *Appl Phys Lett* 70:1480–1482.
11. Wu GT, Weng CS, Zhang XB, Yang HS, Qi ZF, He PM, Li WZ (1999) *J Electrochem Soc* 146:1696–1701.
12. Che GL, Lakshmi BB, Fisher ER, Martin CR (1998) *Nature* 393:346–349.
13. Endo M, Kim YA, Hayashi T, Nishimura K, Matusita T, Miyashita K, Dresselhaus MS (2001) *Carbon* 39:1287–1297.
14. Frackowiak E, Gautier S, Gaucher H, Bonnamy S, Beguin F (1999) *Carbon* 37:61–69.
15. Frackowiak E, Metenier K, Bertagna V, Beguin F (2000) *Appl Phys Lett* 77:2421–2423.
16. Frackowiak E (2007) *Phys Chem Phys* 9:1774–1785.
17. Welton T (1999) *Chem Rev* 99:2071–2083.
18. Swatloski RP, Spear SK, Holbrey JD, Rogers RD (2002) *J Am Chem Soc* 124:4974–4975.
19. Howlett PC, MacFarlane DR, Hollenkamp AF (2004) *Electrochem Solid-State Lett* 7:A97–A101.
20. Kim YJ, Matsuzawa Y, Ozaki S, Park KC, Kim C, Endo M, Yoshida H, Masuda G, Sato T, Dresselhaus MS (2005) *J Electrochem Soc* 152:A710–A715.
21. Murugesan S, Mousa S, Vijayaraghavan A, Ajayan PM, Linhardt RJ (2006) *J Biomed Mater Res B* 79B:298–304.
22. Conway BE, Pell WG (2003) *J Solid State Electrochem* 7:637–644.
23. Lee KB (2005) *J Micromech Microeng* 15:S210–S214.
24. Sato K (1977) *Rev Physiol Biochem Pharmacol* 79:51–131.
25. Nelson PA, Owen JR (2003) *J Electrochem Soc* 150:A1313–A1317.
26. Amatucci GG, Badway F, Pasquier AD, Zheng T (2001) *J Electrochem Soc* 148:A930–A939.
27. Anani AA, Wu H, Lian KK (2000) US Patent 6,117,585.

Downloaded at Palestinian Territory, occupied on December 13, 2021

www.manaraa.com